Ultracold Collisions Observed in Real Time

S. D. Gensemer and P. L. Gould

Department of Physics, U-46, University of Connecticut, Storrs, Connecticut 06269-3046

(Received 5 September 1997)

In laser-induced collisions between ultracold atoms, the combination of low velocities and long-range interactions results in collision times which can exceed the excited-state lifetime. We use a cooperative effect between two lasers to explicitly observe this time dependence. The first laser, tuned near resonance, excites the atom pair at long range and enhances the collisional flux available for short-range excitation by a second, far-detuned laser. Using pulsed excitation, we find this collisional process to take place on a 10^{-6} s time scale, in reasonable agreement with trajectory simulations. [S0031-9007(97)05219-8]

PACS numbers: 34.50.Rk, 32.80.Pj

The ability to follow microscopic systems in real time has become an increasingly important factor in providing information on the system dynamics. Since the relevant time scale is typically quite short (e.g., $<10^{-12}$ s for molecules), extremely fast probes (e.g., ultrafast lasers) are usually required. However, with ultracold atoms (e.g., $T < 1$ mK), the time scale for interactions can be much longer. Obviously, the low atomic velocity is one contributing factor. The other, less obvious aspect is the fact that extremely long-range interatomic potentials can dominate the interactions between these nearly stationary atoms, leading to a greatly increased length scale. We report here our observations of the temporal dynamics of collisions between ultracold atoms occurring on the submicrosecond time scale. Our measurements can be viewed as a stroboscopic following of these very slow collisions in real time.

A great deal of related work has been done on much faster time scales. Transition-state dynamics and chemical reactions have been probed using femtosecond lasers [1,2], and bound molecular wave packets have been created and followed in real time using femtosecond pump-probe techniques [3,4] or time- and frequency-resolved spontaneous emission [5]. Trajectories of continuum wave packets for dissociating molecules (half collisions) have been followed with picosecond resolution via Coulomb explosion [6], and photoassociation, the formation of bound molecules using light, has been observed to occur on the femtosecond time scale at room temperature [7]. In atomic collision studies at room temperature, collision times on the order of a picosecond were inferred from the dependence of the collision rate on laser pulse duration [8].

There has been some limited work performed on slower time scales. Subnanosecond wave packet dynamics of ultracold photoassociative ionization has been discussed [9], and time-dependent studies of cold-atom photoassociation have revealed a long-lived ($\sim 10^{-6}$ s) shape resonance in the scattering of cold ground-state atoms [10]. Also, resonant energy-transfer collisions between velocity-selected Rydberg atoms have been observed to take place on the microsecond time scale [11].

In the present Letter, we investigate the temporal evolution of collisions involving laser-excited ultracold atoms. This brings into play the extremely long-range (R^{-3}) resonant dipole interaction between ground- and excited-state atoms. At low temperatures, this potential energy can greatly exceed the typical kinetic energy even for internuclear separations $R > 100$ nm. Combining this extensive length scale with the low initial atomic velocities ($v \sim 10$ cm/s), we find a collisional time scale in the 10^{-6} s range. This is to be contrasted with collisions at room temperature ($v < 10^3$ m/s) where the atomic trajectories are not affected until $R < 1$ nm, yielding typical collision times on the order of 10^{-12} s. Obviously, in the ultracold case, collision times can exceed the excited-state lifetime ($\sim 10^{-8}$ s), meaning that spontaneous decay can occur during the course of the collision. This fact, coupled with the long range of the interactions and the low atomic kinetic energies, has led to a great deal of interest in the area of ultracold collisions [12–15]. Understanding these collisions is also important because they can be a density-limiting mechanism for laser-cooled atomic samples which are used in various applications (e.g., Bose-Einstein condensation).

In our experiment, we use a pump-probe arrangement with two separate lasers to follow the collisional trajectories in real time. Our signal is based on the flux enhancement effect which we have recently observed in steady state [16]. As shown in Fig. 1(a), one laser (the trap laser) is tuned close to the atomic resonance [detuned by $\Delta_t = -\Gamma_A$ where $\Gamma_A = 2\pi(5.89\ \text{MHz})$ is the atomic decay rate], thereby exciting atom pairs to the attractive $C_3 R^{-3}$ potential at very long range [Condon radius $R_t = (\frac{C_3}{\hbar \Delta_t})^{1/3}$]. Since the atoms are initially moving so slowly, and their acceleration is small, spontaneous decay occurs before the atoms approach closely enough for an inelastic trap loss process [e.g., radiative escape (RE) or a fine-structure change (ΔJ)] to occur [17]. In other words, the excitation does not survive to short range. Although no observable trap loss collision occurs, the trajectories are significantly affected. In particular, the deflections result in an enhanced ground-state collisional

 0031-9007/98/80(5)/936(4)$15.00

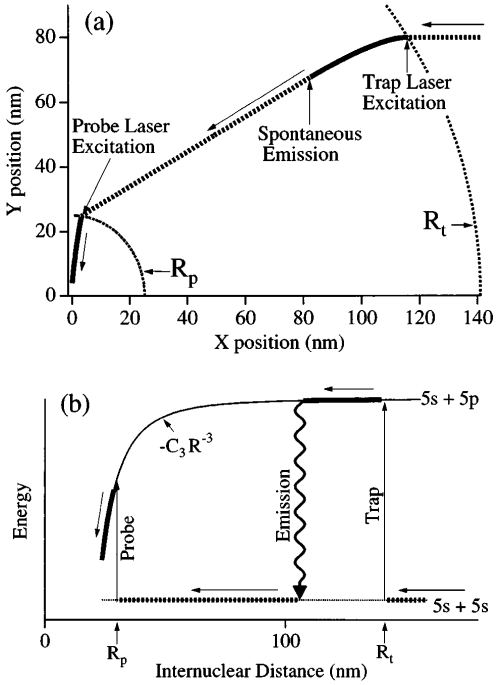

FIG 1. (a) Typical classical trajectory of an atomic collision showing the flux enhancement effect. The solid (dashed) line indicates the atom's trajectory while in the excited (ground) state. The incoming atom approaches from the right. The atom pair is excited at R_t by the trap laser pulse and is accelerated by the attractive long-range potential. After spontaneous decay, it proceeds to R_p, where it may be excited again by a probe laser pulse. The atom pair is then accelerated quickly into short range, where either RE or ΔJ may occur, leading to trap loss. (b) Molecular potential diagram for the same process.

flux available for the second (probe) laser which is tuned farther below the atomic resonance ($|\Delta_p| \gg \Gamma_A$) and capable of exciting atom pairs at shorter range ($R_p < R_t$). Atom pairs excited by the probe laser are quickly accelerated by the steeper attractive potential and are much more likely to undergo an inelastic trap loss collision. However, the rate of collisions induced by this laser alone is relatively low, because its smaller R_p results in less collisional flux intercepted. The two lasers, acting in concert, yield a relatively high rate of collisions, i.e., the trap laser provides an enhanced flux which the probe laser causes to collide efficiently. The key point of the present paper is that this flux enhancement effect takes place on a rather long time scale; i.e., the atoms travel slowly from R_t to R_p. We observe this by pulsing the two excitations and measuring the enhanced collision rate as a function of delay between the pulses.

We have performed semiclassical numerical calculations of the distribution of collision times for the parameters of our experiment. In these simulations, we calculate the collision time (i.e., the time to travel from R_t to R_p) for an atom pair with initial impact parameter b_i and relative velocity v_i. The atom pair is assumed to interact with the trap laser only at R_t; i.e., off-resonant excitation is ignored. The excitation process is calculated as a Landau-Zener probability using the atomic Rabi rate divided by $\sqrt{3}$ (to account for directional averaging [16,18]). The classical trajectory [Fig. 1(a)] of the excited atoms under the influence of the attractive potential is followed until spontaneous emission at time t_e returns the atom pair to the ground state ($5s_{1/2} + 5s_{1/2}$) potential, which is assumed to be flat. Therefore, the velocity and time of arrival at R_p, where the second excitation occurs, are calculated assuming a straight line trajectory after the spontaneous decay from the first excitation. The probability of excitation at R_p by the probe laser is also calculated as a Landau-Zener process. The survival after the second (probe) excitation is not an issue. The starting radius is sufficiently small and the attractive potential sufficiently steep that an excited atom makes it all the way into short range, where the inelastic trap loss process occurs, before decaying.

Trajectories will have different collision times depending on the values of b_i, v_i, and t_e. Therefore we average over these parameters (weighted by their normalized distribution functions P_v, P_b, and P_{t_e}) to arrive at the distribution of collision times,

$$f(t_{\rm coll}) = \int_{v_i=0}^{\infty} dv_i\, P_v \int_{b_i=0}^{\infty} db_i\, P_b P_{\rm LZt}(v_i, b_i) \times [1 - P_{\rm LZp}(v_i, b_i)] \int_{t_e=0}^{\infty} dt_e\, P_{t_e} P_{\rm LZp}(v_f, b_f) \times \delta(t'_{\rm coll} - t_{\rm coll}), \quad (1)$$

where

$$P_v = \frac{M}{2kT} v_i e^{-v_i^2(M/4kT)},$$

$$P_b = 2b_i/R_t^2,$$

and

$$P_{t_e} = e^{-t_e/\tau}/\tau.$$

Here τ is the (R-dependent) molecular excited-state lifetime, M is the reduced mass, T is temperature, and $t'_{\rm coll}$ is the total time from R_t to R_p for a molecule that spends time t_e in the excited state. $P_{\rm LZt}$ and $P_{\rm LZp}$ are the excitation probabilities due to trap and probe lasers, respectively, using the Landau-Zener formula in the dressed-atom picture [15]. The factor $[1 - P_{\rm LZp}(v_i, b_i)]$ in (1) takes account of the fact that in our experiment we measure the difference between inelastic collision rates with both lasers on and with the probe laser on alone, so the effect of the probe laser alone must be factored out of the simulation. We assume delta-function trap and probe pulses. The hyperfine structure is ignored and detunings are referenced to the $5s_{1/2}(F = 3) + 5p_{3/2}(F' = 4)$ asymptote for ^{85}Rb.

The five curves in Fig. 2 are plots of $f(t_{\rm coll})$ for each of the five attractive [Hund's case (c)] molecular states of the Rb atom which are optically coupled to the ground state [17]. Clearly each of these states, characterized by different C_3 coefficients (ranging from $0.442d^2$ for 1_u to $1.667d^2$ for 0_u^+, where $d^2 = 10.1e^2a_0^2$ is the square of the dipole

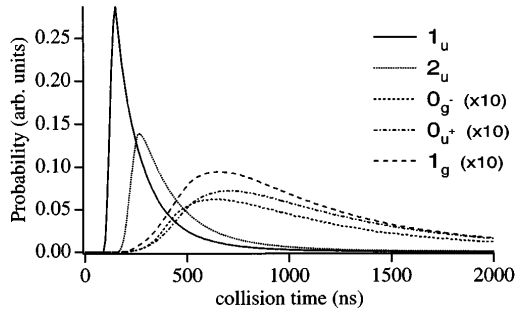

FIG 2. Classical simulations of time-resolved collisions at $T = 50\ \mu$K. The trap (probe) laser intensity and detuning are 15.2 mW/cm^2 (7 W/cm^2) and -1Γ (-169Γ), respectively. The five curves are generated using the C_3 coefficients and excited-state lifetimes for each of the Hund's case (c) attractive molecular states. Plotted is the probability for flux enhancement to take place as a function of collision time (i.e., time to travel from R_t to R_p).

matrix element) and lifetimes (ranging from $0.500\tau_A$ for 0_g^- to $1.850\tau_A$ for 1_u, where $\tau_A = 27$ ns is the atomic lifetime), will contribute a different distribution of collision times to the total measured. In particular, the 1_u and 2_u states, which have the longest excited-state lifetimes, contribute significantly more to the flux enhancement than the other three states and have considerably shorter collision times. This is due to the improved survival (after the first excitation) of these longer-lived states and the larger radial velocity (and hence greater deflection) obtained during their longer lifetime on the attractive excited potential. In fact, the simulations show that the lifetime is much more important than the C_3 coefficient in determining the distribution of collision times. Another fact which emerges is that the energy gained as a result of the first excitation is typically rather small, indicating that the decay does indeed occur at long range, causing the atoms to travel most of the way from R_t to R_p in the ground state. As we would expect, simulations at higher temperatures yield shorter average collision times. We note that the 2_u state is coupled to the ground state only through retardation effects [17]. Its lifetime is therefore strongly dependent on R (infinite at short range), a fact which is included in the simulations.

The experiment is performed by measuring the laser-induced collisional decay rate of ^{85}Rb atoms confined in a magneto-optical trap [19] (MOT). The trap and probe lasers are detuned by $\Delta_t = -1\Gamma$ and $\Delta_p = -169\Gamma$ from the $5s_{1/2}(F = 3) \rightarrow 5p_{3/2}(F' = 4)$ atomic resonance at 780 nm. The probe laser passes through the MOT at 45° between the two radial MOT trapping beams, with a $\frac{1}{e}$ diameter roughly twice that of the atom cloud. The probe laser is circularly polarized and retroreflected to create a uniform intensity $\sigma^+ - \sigma^-$ laser field with a total intensity of 7 W/cm^2. The trap laser intensity is fixed at 3.8 mW/cm^2, resulting in a very small trap-laser-induced collisional loss rate $\beta_t < 10^{-13}$ cm^3 s^{-1}, due to the low-temperature suppression effect [20]. Keeping this low background β is crucial to accurately measuring small changes, β_p, induced by the probe laser. Both lasers are chopped by acousto-optic modulators with a 10% $\rightarrow$ 90% rise time of 30 ns. Other details of the trap parameters can be found in [16]. The temperature of the atoms at the intensity and detuning we use was previously [21] measured to be $\sim 50\ \mu$K.

The timing scheme for the experiment is shown in Fig. 3(a). The trap laser is chopped with a 10 μs period and a 50% duty cycle. During the 5 μs cooling-trapping phase, the trap laser is on at low intensity (3.8 mW/cm^2) to keep the atoms cooled and maintain the trap depth. During the 5 μs probe phase, a more intense (15.2 mW/cm^2) 100 ns (FWHM) trap laser pulse is applied, followed, after a variable delay δ, by a 100 ns probe laser pulse. This sequence is repeated 5 times, once every 1 μs, during the probe phase.

To measure the increase in the trap loss collision rate constant (β), we measure it with only the trap laser on (β_t), then with both trap and probe lasers on (β_{t+p}). We then define $\beta_p = \beta_{t+p} - \beta_t$. By subtracting β_t, we ensure that any systematic errors produced by small changes in laser alignment, trap laser intensity, excited-state fraction, or density of the atom cloud will be reduced.

Experimental results are shown in Fig. 3(b) where β_p is plotted as a function of pulse delay. As can be seen, there is a well-defined peak in the time-dependent signal, characteristic of the transit time between the two laser

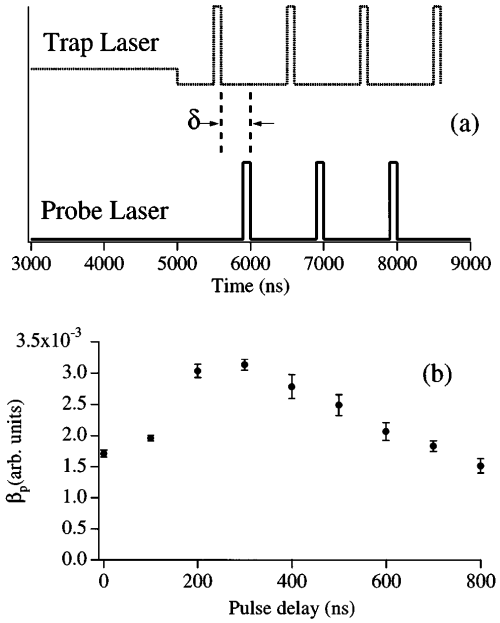

FIG 3. (a) Timing of the trap and probe laser pulses for the experiment. The trap laser is on at low (3.8 mW/cm^2) intensity for 5 μs. This is followed by a series of short (100 ns), intense (15.2 mW/cm^2) trap pulses. The probe pulses are 100 ns long and are peaked at time δ after the peak of each trap pulse. The entire pattern repeats every 10 μs. (b) β_p plotted as a function of δ. The flux enhancement effect increases only after a delay of 200 ns, indicating a minimum collision time of $\sim$200 ns. It then drops off slowly, in reasonable agreement with the simulations (Fig. 2).

excitations at long and short range. There are essentially no enhanced collisions until a delay of 200 ns. The curve then rises steeply and falls off slowly for long delays. This behavior is consistent with the predictions of the simulations (Fig. 2), in particular, the contributions of the the 1_u and 2_u potential curves, indicating the importance of long-lived molecular states to the trap loss process. There is a rate of inelastic collisions which is independent of delay, which, of course, are those collisions induced by the probe laser without any enhancement by the trap laser.

It is difficult for us to quantitatively compare our measurements and simulations because hyperfine structure and nonadiabatic effects significantly influence evolution on the interatomic potentials near the atomic asymptotes [22,23]. In fact, near-resonant trap-loss collisions in general are not well understood, although long-lived states, such as the 2_u, are thought to play an important role [17,24,25]. In our case, we are mainly concerned with the attractive potentials which converge to the $F = 3 + F' = 4$ limit. According to our simulations, most atom pairs excited by the trap laser decay at long range, i.e., before encountering the myriad of hyperfine curve crossings. This is true even for long-lived states, e.g., 90% of the 1_u excitations (which would contribute to our flux enhancement signal) decay before reaching $R = 36$ nm (cf. $R_t = 72$ nm, $R_p = 13$ nm) and thus gain less than $7\hbar\Gamma$ of energy. This is to be compared to the $\sim 20\hbar\Gamma$ splitting between the $F' = 3$ and $F' = 4$ excited-state hyperfine levels. Although the Hund's case (c) labels no longer apply in this hyperfine-dominated regime, there undoubtedly exist attractive states which are long lived at large R. As can be seen in comparing Figs. 2 and 3, these potentials appear to contribute significantly to our signal.

In future experiments, measurements of collisional time evolution for different detunings of the initial excitation and for different atomic asymptotes may help sort out the roles of the various hyperfine curves. In fact, our simulations indicate that the flux enhancement factor can be larger (because of improved survival) for increased trap laser detunings. A time-dependent flux enhancement may also prove useful for investigating collisional processes which use time-resolved (e.g., ionization) detection. Better time resolution will also allow the use of enhanced flux arriving on excited as well as ground-state potentials.

In conclusion, we have demonstrated a novel technique for the study of ultracold collisions in the time domain. These time-resolved collisions yield information complementary to that obtained from photoassociative or trap loss spectra. In general, spectral information is better suited for processes occurring on fast time scales, e.g., molecular vibrations (measured by vibrational spacings) and predissociation rates (measured by linewidths). However, the spectral resolution, especially near the atomic limit, is usually not sufficient to reveal dynamics on the submicrosecond time scale, such as those responsible for the trap loss collisions we have investigated here. The present results are not only a striking demonstration of the ability to follow these slow collisions in real time, but have already yielded useful information concerning the importance of long-lived molecular states to the trap loss process.

We acknowledge technical assistance from S. Ciris and useful discussions with E. Tiesinga regarding the effects of hyperfine structure on the long-range molecular potentials. This work was supported in part by the Division of Chemical Sciences, Office of Basic Energy Sciences, Office of Energy Research, U.S. Department of Energy. S. G. acknowledges financial support from the Connecticut Space Grant College Consortium.

[1] A. H. Zewail, Faraday Discuss. Chem. Soc. **91**, 207 (1991).
[2] A. H. Zewail, J. Phys. Chem. **100**, 12 701 (1996).
[3] R. H. Bowman, M. Dantus, and A. H. Zewail, Chem. Phys. Lett. **161**, 297 (1989).
[4] T. Baumert, M. Grosser, R. Thalweiser, and G. Gerber, Phys. Rev. Lett. **67**, 3753 (1991).
[5] T. J. Dunn, J. N. Sweetser, I. A. Walmsley, and C. Radzewicz, Phys. Rev. Lett. **70**, 3388 (1993).
[6] H. Stapelfeldt, E. Constant, and P. B. Corkum, Phys. Rev. Lett. **74**, 3780 (1995).
[7] U. Marvet and M. Dantus, Chem. Phys. Lett. **245**, 393 (1995).
[8] T. Sizer II and M. G. Raymer, Phys. Rev. Lett. **56**, 123 (1986).
[9] M. Machholm, A. Giusti-Suzor, and F. H. Mies, Phys. Rev. A **50**, 5025 (1994).
[10] H. M. J. M. Boesten, C. C. Tsai, B. J. Verhaar, and D. J. Heinzen, Phys. Rev. Lett. **77**, 5194 (1996).
[11] D. S. Thomson, M. J. Renn, and T. F. Gallagher, Phys. Rev. Lett. **65**, 3273 (1990).
[12] P. Julienne, A. M. Smith, and K. Burnett, Adv. At. Mol. Opt. Phys. **33**, 141 (1993).
[13] T. Walker and P. Feng, Adv. At. Mol. Opt. Phys. **34**, 125 (1994).
[14] J. Weiner, Adv. At. Mol. Opt. Phys. **35**, 45 (1995).
[15] K.-A. Suominen, J. Phys. B **29**, 5981 (1996).
[16] V. Sanchez-Villicana, S. D. Gensemer, and P. L. Gould, Phys. Rev. A **54**, R3730 (1996).
[17] P. Julienne and J. Vigue, Phys. Rev. A **44**, 4464 (1991).
[18] P. L. DeVries and T. F. George, Mol. Phys. **36**, 151 (1978).
[19] E. L. Raab *et al.*, Phys. Rev. Lett. **59**, 2631 (1987).
[20] C. D. Wallace, V. Sanchez-Villicana, T. P. Dinneen, and P. L. Gould, Phys. Rev. Lett. **74**, 1087 (1995).
[21] C. D. Wallace *et al.*, J. Opt. Soc. Am. B **11**, 703 (1994).
[22] C. J. Williams and P. S. Julienne, J. Chem. Phys. **101**, 2634 (1994).
[23] T. Walker and D. E. Pritchard, Laser Phys. **4**, 1085 (1994).
[24] L. Marcassa *et al.*, Phys. Rev. A **47**, R4563 (1993).
[25] P. D. Lett *et al.*, J. Phys. B **28**, 65 (1995).